2009 American Control Conference
Hyatt Regency Riverfront, St. Louis, MO, USA
June 10-12, 2009

A Nested PID Steering Control for Lane Keeping in Vision Based Autonomous Vehicles

Riccardo Marino*, Stefano Scalzi*, Giuseppe Orlando*, Mariana Netto**

Abstract— **In this paper a nested PID steering control for lane keeping in vision based autonomous vehicles is designed to perform path following in the case of roads with an uncertain curvature. The control input is the steering wheel angle: it is designed on the basis of the yaw rate, measured by a gyroscope, and the lateral offset, measured by the vision system as the distance between the road centerline and a virtual point at a fixed distance from the vehicle. No lateral acceleration and no lateral speed measurements are required. A PI active front steering control on the yaw rate tracking error is used to reject constant disturbances and the overall effect of parameter variations while improving vehicle steering dynamics. The yaw rate reference is viewed as the control input in an external control loop: it is designed using a PID control on the lateral offset to reject the disturbances on the curvature which increase linearly with respect to time. The robustness is investigated with respect to speed variations and uncertain vehicle physical parameters: it is shown that the controlled system is asymptotically stable for all perturbations in the range of interest. Several simulations are carried out on a standard big sedan CarSim vehicle model to explore the robustness with respect to unmodelled effects such as combined lateral and longitudinal tire forces, pitch and roll. The simulations show reduced lateral offset and new stable μ-split braking manoeuvres in comparison with the CarSim model predictive steering controller implemented by CarSim.**

I. Introduction

Intelligent vehicles and automated highway systems have attracted a growing attention in the last years with the aim of increasing safety and comfort: see for instance [1], [2], [3], [4], [5], [6], [7], [8], [9], [10], [11], [12], [13], [14], [15] and [16]. In [1], [2] a feedback from lateral and longitudinal vehicle speed, yaw angle error and yaw rate is used to help the driver to steer the vehicle back to the lane during diminished driving capability due to inattention. The control strategy is based on the Lyapunov theory and LMI optimization by defining polytopic and hypercubic state space regions, where if the driver stays in, the driving task is considered safe; the main idea is to approximate these regions by standard and composite Lyapunov level curves. In [3] a H_∞ controller is designed to minimize the effect of the disturbances on the measured lateral offset and the desired yaw angle. In [4] a steering controller, which uses finite preview optimal control methods, is proposed to control the measured lateral offset, the yaw angle and their derivatives. In [5] a closed loop control strategy which feeds back the lateral offset is proposed: an automatic lane keeping is combined with the driver's steering with no need of switching strategies between the driver and the lane keeping control. In [6] a control system based on the loop shaping technique is tested by experiments using a feedback from the lateral offset. In [7] a non linear observer based control strategy is investigated by measuring the lateral offset, its derivative, the yaw angle and the yaw rate. In [8] a model predictive steering controller is used to emulate the driver behaviour in the CarSim environment: it is designed on the basis of a simplified linear model and on longitudinal and lateral speed, yaw angle and yaw rate measurements to predict the error with respect to a given target path. Also in [9] a model predictive control approach is followed: the controlled outputs are the lateral offset, the yaw rate and the yaw angle; the controller is designed both on a nonlinear and a linear vehicle model using lateral and longitudinal vehicle speed, yaw angle and yaw rate measurements. In [10] a feed forward and a feedback action on the lateral offset and the yaw angle error is experimented. In [11] a gain scheduling based proportional feedback from the lateral offset is experimented. In [12] a feed forward term from road curvature and a PID on a weighted sum of the heading error and the lateral offset are used as steering controller in the DARPA Grand Challenge. In the same competition the yaw angle and a nonlinear term proportional to the lateral offset are used in [13] as measurements to design the steering controller. Furthermore, to improve safety, driver comfort and vehicle performance, several driver assistance systems are investigated in the literature. In [14] a steering assistance control system with a feedback from the lateral offset and lateral speed is designed to follow the desired path while an assistance torque is applied in order to improve the vehicle handling and steering feel. In [15] and [16] the active front steering is proposed and implemented on BMW 5 Series vehicle. In [15] a PI active front steering control on the yaw rate tracking error with different gains for braked and unbraked driving condition is used while in [16] a patented method is proposed to ensure safety during active steering system failure computing the steering wheel angle as the sum of the proposed control law steering angle and the driver steering angle. Most control algorithms employed in lane keeping make use of pole placement, model predictive and observer based techniques or require difficult measurements

*University of Rome Tor Vergata, Electronic Engineering Department - Via del Politecnico 1, 00133 Roma - Italy, Tel. 0039 06 7259 7412. email: {marino, scalzi}@ing.uniroma2.it

**LCPC/INRETS - LIVIC Vehicle-Infrastructure-Driver Interactions Research Unit, 14 Route de la miniére, 78000 Versailles, France.

978-1-4244-4524-0/09/$25.00 ©2009 AACC

of lateral speed, vehicle absolute position and orientation. The simplest algorithm [11] only implements a proportional feedback from the lateral offset; since in addition to lateral offset measurements from vision systems the yaw rate measurements are easily obtained by an on board gyroscope, in this paper we propose a control scheme which integrates the active steering action based on the yaw rate error with the lane keeping action based on lateral offset. A nested PID steering control for lane keeping in vision based autonomous vehicles is designed to perform path following in the case of roads with a curvature which increases linearly with respect to time. No lateral speed measurement is used since it can be hardly measured with high cost and low accuracy and reliability. The control input is the steering wheel angle: it is designed on the basis of the yaw rate measured by a gyroscope and the lateral offset measured by the vision system as the distance between the road centerline and a virtual point at a fixed distance from the vehicle. A PI active front steering control on the yaw rate tracking error is used to reject constant disturbances and the effect of uncertain parameters while improving vehicle steering dynamics. To integrate the additional lateral offset measure the yaw rate reference is viewed as the control signal in an external control loop: it is designed using a PID control (with an additive double integral action) on the lateral offset to reject the disturbances on the curvature which increase linearly with respect to time. The robustness is proved, by using the theorem presented in [18], [19], with respect to speed variation and uncertainties on vehicle physical parameters such as the front and rear cornering stiffnesses and the vehicle mass. It is shown how the robustness of the controlled system decreases as speed increases. The asymptotical stability is however ensured for all perturbations in the range of interest. Several simulations, such as the tracking of a CarSim environment default path and a standard sudden braking action on surfaces with different adherence conditions (μ-split braking manoeuvre), are carried out on a standard big sedan CarSim vehicle model to explore the robustness with respect to unmodelled effects, such as combined lateral and longitudinal tire forces, pitch and roll. The simulations show reduced lateral offset and new stable μ-split braking manoeuvres with respect to the CarSim model predictive steering controller which requires lateral speed.

II. Vehicle model

A detailed standard big sedan CarSim vehicle model is used in numerical simulations to analyze the responses of both the uncontrolled and the controlled vehicle. CarSim vehicle uses nonlinear tire models according to combined sideslip theory [20], nonlinear spring models, and incorporates the major kinematics and compliance effects in the suspensions and steering systems including differential load transfer for each wheel. However, to design the controller, a widely used simplified single track vehicle model [17] is considered which captures the essential vehicle steering dynamics:

$$\begin{aligned} m(\dot{v}_x - r v_y) &= f_{lf}\cos\delta_f + f_{sf}\sin\delta_f + f_{lr} \\ m(\dot{v}_y + r v_x) &= f_{lf}\sin\delta_f - f_{sf}\cos\delta_f - f_{sr} \\ J\dot{r} &= l_f(f_{lf}\sin\delta_f - f_{sf}\cos\delta_f) + l_r f_{sr} \end{aligned} \tag{1}$$

$$f_{si}(\alpha_i) = D\sin\{C\,\mathrm{atan}[(1-E)B\alpha_i + E\,\mathrm{atan}(B\alpha_i)]\} \tag{2}$$

$$\alpha_f = \tfrac{v_y + l_f r}{v_x} - \delta_f, \qquad \alpha_r = \tfrac{v_y - l_r r}{v_x} \tag{3}$$

$$v_y = v\sin\beta \tag{4}$$

where f_{si}, with $i = f, r$, are the front and rear lateral forces and f_{li}, $i = f, r$ are the front and rear longitudinal forces which are modelled according to Pacejka tire model, [20]. The tire sideslip angle and consequently the sign of the lateral forces are computed as in (3) according to CarSim tire model (SAE ISO standard, see [20]). All variables and parameters are defined in the appendix (Table I).

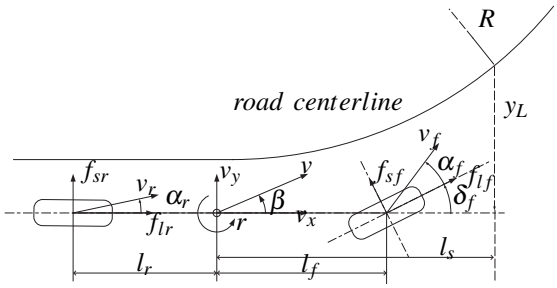

Fig. 1. Single track vehicle model

The CCD camera measures the lateral deviation of the front preview point y_L that can be modeled [1] as follows:

$$\dot{y}_L = \beta v + l_s r + v\psi \tag{5}$$

where ψ is the yaw angle and y_L is the lateral offset from the road centerline at a preview distance l_s (see Fig. 1).
The system (1) is linearized about uniform rectilinear motion ($v_x = v =$constant, $r = 0$, $v_y = 0$, $\delta_f = 0$): the longitudinal dynamics is decoupled from the lateral dynamics and can be neglected as far as the steering dynamics are concerned. The reduced linear system, $\dot{x} = Ax + Bu$, which includes the lateral offset dynamics (5) is given by:

$$\begin{bmatrix} \dot{\beta} \\ \dot{r} \\ \dot{\psi} \\ \dot{y}_L \end{bmatrix} = \begin{bmatrix} a_{11} & a_{12} & 0 & 0 \\ a_{21} & a_{22} & 0 & 0 \\ 0 & 1 & 0 & 0 \\ v & l_s & v & 0 \end{bmatrix} \begin{bmatrix} \beta \\ r \\ \psi \\ y_L \end{bmatrix} + \begin{bmatrix} b_1 \\ b_2 \\ 0 \\ 0 \end{bmatrix} \delta_f + \begin{bmatrix} 0 \\ 0 \\ -v \\ 0 \end{bmatrix} \rho \tag{6}$$

where ρ is the road curvature defined as $\rho = 1/R$, with R the curvature radius. The coefficients appearing in systems (6), which may depend on v and on uncertain physical parameters are:

$$\begin{array}{ll} a_{11} = -\frac{(c_f+c_r)}{mv}, & a_{12} = -1 - \frac{(c_f l_f - c_r l_r)}{mv^2}, \\ a_{21} = -\frac{(c_f l_f - c_r l_r)}{J}, & a_{22} = -\frac{\left(c_f l_f^2 + c_r l_r^2\right)}{Jv}, \\ b_1 = \frac{c_f}{mv}, & b_2 = \frac{c_f l_f}{J}, \end{array} \tag{7}$$

where c_f and c_r are the front and the rear tire cornering stiffness which are the linear approximation of (2). The vehicle parameters for the simplified single track vehicle model (6), whose values are identified from a big sedan CarSim vehicle model, are given in Appendix (Table II).

III. Control strategy

A. Control design

The proposed control strategy is illustrated in Fig. 2. It involves the design of two nested control blocks. The first one, called C_1, has to ensure the tracking of a yaw rate reference signal on the basis of the yaw rate tracking error in spite of constant disturbances and parameters uncertainties while the second one, called C_2, has to generate the yaw rate reference signal on the basis of the lateral offset. The task of C_1 is to steer to zero the difference between the measured yaw rate r and desired yaw rate r_d.

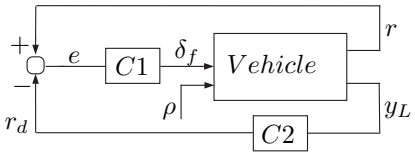

Fig. 2. Controlled system scheme

Following the active steering approach in [15] a PI control has been used for C_1:

$$\begin{array}{l} C1:\ \delta_f = -K_{P1}(r - r_d) - K_{I1}\int_0^t (r - r_d)\, d\nu \\ \qquad = -K_{P1}(r - r_d) - K_{I1}\alpha_0. \end{array} \tag{8}$$

where α_0 is the additional state introduced by the dynamic control (8). The feedback from the yaw rate r improves the transients, by changing the eigenvalues displacement, of the steering dynamics. Substituting (8) in (6) we obtain:

$$\dot{x}_{as} = \begin{bmatrix} a_{11} & a_{12} - K_{P1}b_1 & 0 & 0 & -b_1 K_{I1} \\ a_{21} & a_{22} - K_{P1}b_2 & 0 & 0 & -b_2 K_{I1} \\ 0 & 1 & 0 & 0 & 0 \\ v & l_s & v & 0 & 0 \\ 0 & 1 & 0 & 0 & 0 \end{bmatrix} x_{as} + \begin{bmatrix} K_{P1}b_1 \\ K_{P1}b_2 \\ 0 \\ 0 \\ -1 \end{bmatrix} r_d + \begin{bmatrix} 0 \\ 0 \\ -v \\ 0 \\ 0 \end{bmatrix} \rho \tag{9}$$

where:

$$x_{as} = [\beta \quad r \quad \psi \quad y_L \quad \alpha_0]^T .$$

Once the regulator C_1 is designed, the key idea is to integrate the additional lateral offset measure considering the yaw rate reference signal r_d in (9) as the control input to be designed to drive the output y_L to zero. Therefore, to design the desired yaw rate reference, it is necessary to model the dynamics of the road curvature, considering it as a disturbance on the lateral offset. In the case of a constant road curvature one integral term is needed to reject the disturbance; since the road curvature, in the case of non trivial manoeuvres, may be considered as increasing linearly with respect to time an additional integral term is necessary and the regulator C_2 becomes:

$$\begin{array}{l} C2:\ r_d = -K_{P2}y_L - K_{I2}\int_0^t y_L\, d\nu \\ \qquad -K_{I3}\int_0^t\int_0^\nu y_L\, d\eta\, d\nu - K_d \dot{y}_{Ld} \\ \qquad = -K_{P2}y_L - K_{I2}\alpha_2 - K_{I3}\alpha_1 - K_d \dot{y}_{Ld}\ . \end{array} \tag{10}$$

where:

$$\dot{\alpha}_1 = y_L, \tag{11}$$

$$\dot{\alpha}_2 = \alpha_1. \tag{12}$$

and the signal y_{Ld} is given by:

$$\dot{\alpha}_3 = -\frac{1}{\tau}\alpha_3 + y_L \tag{13}$$

$$y_{Ld} = -\frac{1}{\tau^2}\alpha_3 + \frac{1}{\tau}y_L \tag{14}$$

where τ is the filter time constant.

The final structure of the control algorithm is shown in Fig. 2 in which C_1 is given by (8) and C_2 is given by (10).

B. Control properties

To choose the six control gains the closed loop linear system (9) and (10) is considered assuming an ideal steering actuator. However the control gains are chosen so that the bandwidth of the transfer function between r_d and δ_f is within a typical actuator bandwidth (about 10 Hz). In order to avoid instability phenomena a derivative term has been added and the integral gains are chosen to be small as suggested in [21]. The derivative term gain is small in order to avoid chattering phenomena; the chosen gains are:

$$\begin{array}{c} K_{P1} = 20; \quad K_{I1} = 10; \quad K_{P2} = 30; \\ K_{I2} = 0.01; \quad K_{I3} = 0.01; \quad K_d = 0.05. \end{array} \tag{15}$$

In conclusion the controlled system (9) and (10) $\dot{x}_c = A_c x_c + B_c \rho$ and the equilibrium point x_{ce} are shown below:

$$A_c = \begin{bmatrix} a_{c11} & a_{c12} & 0 & a_{c14} & a_{c15} & a_{c16} & a_{c17} & a_{c18} \\ a_{c21} & a_{c22} & 0 & a_{c24} & a_{c25} & a_{c26} & a_{c27} & a_{c28} \\ 0 & 1 & 0 & 0 & 0 & 0 & 0 & 0 \\ v & l_s & v & 0 & 0 & 0 & 0 & 0 \\ 0 & 1 & 0 & a_{c54} & 0 & a_{c56} & a_{c57} & a_{c58} \\ 0 & 0 & 0 & 1 & 0 & 0 & 0 & 0 \\ 0 & 0 & 0 & 0 & 0 & 1 & 0 & 0 \\ 0 & 0 & 0 & 1 & 0 & 0 & 0 & -\frac{1}{\tau} \end{bmatrix}$$

$$B_c = \begin{bmatrix} 0 & 0 & -v & 0 & 0 & 0 & 0 & 0 \end{bmatrix}^T \quad (16)$$

with

$$x_c = \begin{bmatrix} \beta & r & \psi & y_L & \alpha_0 & \alpha_1 & \alpha_2 & \alpha_3 \end{bmatrix}^T \quad (17)$$

$$x_{ce} = -\begin{bmatrix} \frac{(b_2a_{12}-b_1a_{22})v}{a_{11}b_2-a_{21}b_1} \\ -v \\ \frac{(a_{42}(a_{11}b_2-a_{21}b_1)+a_{41}(b_1a_{22}-b_2a_{12}))v}{a_{43}(a_{11}b_2-a_{21}b_1)} \\ 0 \\ -\frac{(a_{11}a_{22}-a_{21}a_{12})v}{K_{I1}(a_{11}b_2-a_{21}b_1)} \\ 0 \\ \frac{v}{K_{I2}} \\ 0 \end{bmatrix} \rho, \quad (18)$$

where τ is set equal to $\tau = 0.01$ and l_s is chosen equal to $l_s = 13\ [m]$ while the parameters a_{cij} are shown in Table III. With the chosen gains (15) the controlled system stability is guaranteed since the poles are on the left hand side of the complex plane. The stability is robust with respect to vehicle parameter variations as shown in the robustness analysis paragraph. Finally the frequency behaviour of the controlled system has been analyzed. In Fig. 3 the behaviour of the controlled system with respect to the road curvature ρ is shown.

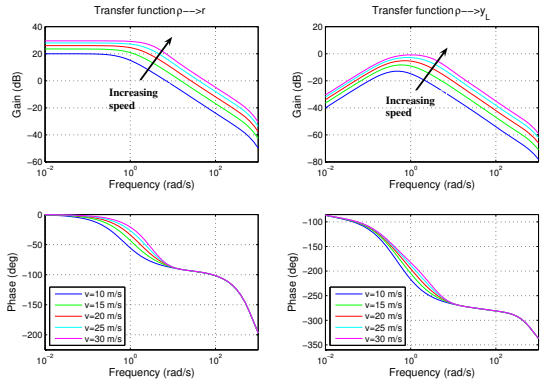

Fig. 3. Bode diagram of the transfer functions between ρ and y_L and ρ and r

On the left hand side of Fig. 3 the transfer function from the road curvature to the yaw rate is shown while, on the right hand side of Fig. 3, the reduction of the road curvature effect on the lateral offset is shown.The transfer function between ρ and y_L for a speed v equal to $v = 36\ m/s$ is computed below to show the double zeros at the origin which ensure the rejection of disturbances that increase linearly with respect to time:

$$y_L = -\frac{36s^2\left(36s^4+45\ 10^3s^3+444\ 10^4s^2+2972\ 10^4s+137\ 10^5\right)}{s^8+h_7s^7+h_6s^6+h_5s^5+h_4s^4+h_3s^3+h_2s^2+h_1s+h_0}\rho; \quad (19)$$

the coefficients h_i are shown in Table IV.

C. Robustness

Only the robustness of the internal loop (Fig. 4) is analyzed since it contains the uncertain parameters of interest c_f, c_r, m and v. As a consequence only the first two dynamical equations in (6) along with (8) are considered for the robustness analysis.

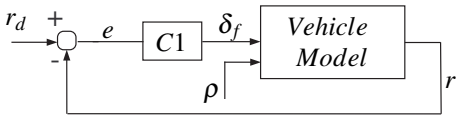

Fig. 4. Internal loop control scheme

We define: Σ_0 as the reduced system containing the dynamics of β and r with unperturbed parameters; Σ as the reduced system with perturbations on c_f, c_r and m, $\Delta_P = P - P_0$ as the perturbation on Σ, where P and P_0 are the perturbed and the nominal transfer functions between the δ_f and r respectively; $V_0 = C_1(1+P_0C_1)^{-1}$ the transfer function between δ_f and r_d as the control sensitivity function; $\bar{\sigma}$ as the operator that gives the greater singular value of a transfer function. We can apply the following theorem.

Theorem 1: [18], [19]

If:

α_0) $\lim_{s\to\infty}(1+P_0C_1) \neq 0$

α_1) Σ_0 is asymptotically stable

then Σ is asymptotically stable for all variations or perturbations of P from P_0 such that:

β) the number of eigenvalues of A in C^- is equal to the number of eigenvalues of A_0 in C^-

γ) $\lim_{s\to\infty}(1+PC_1) \neq 0$

δ) $\bar{\sigma}\left[\Delta_P(\omega)\right] < \frac{1}{\bar{\sigma}[V_0(\omega)]}, \forall\omega \in$ Imaginary axis.

Theorem 1 is satisfied for different speeds and perturbations on tire parameters such as the cornering stiffnesses c_r, c_f (which may change due to different adherence conditions and/or low tire pressure) and the vehicle mass m (that varies from unloaded to full load conditions). The robustness decreases as speed increases as shown in the Fig. 5, in which a speed variation from 1 m/s to 36 m/s is considered. On the Y-axis of Fig. 5 an upper bound for the percentage variations of all the parameters c_r, c_f and m for which the robustness guarantees the asymptotic stability of Σ is shown.

IV. CarSim simulations

Several simulations in CarSim environment have been performed to compare the CarSim driver model, which is based on a model predictive control system [8] and makes

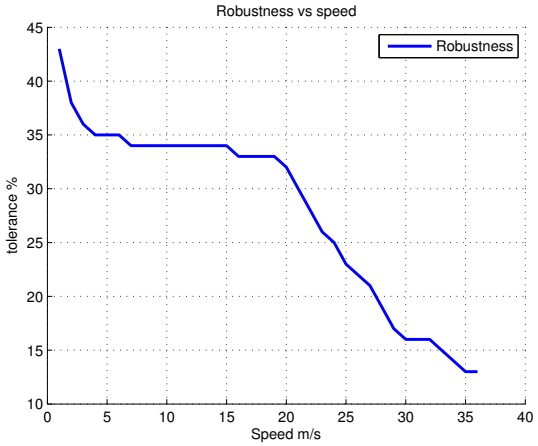

Fig. 5. Robustness with respect to increasing speed

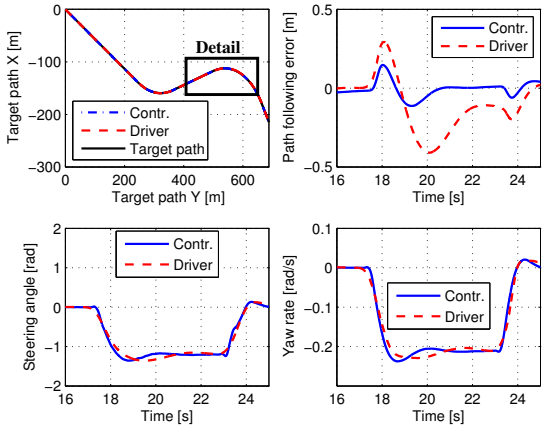

Fig. 6. Standard CarSim path following manoeuvre ($v = 31\ [m/s]$)

also use of vehicle lateral speed, with the proposed nested PID control. CarSim vehicle uses detailed nonlinear tire models according to combined slip theory and takes into account the major kinematics and compliance effects of the suspensions (nonlinear spring models) and steering systems. The vehicle has a nonlinear second order speed depending rack and pinion ratio steering system; for the active steering a realistic actuator with a bandwidth of 10Hz is considered. The first simulation, shown in Fig. 6, concerns a path following in the case of a typical highway road curvature profile at a vehicle speed of 31 $[m/s]$. In Fig. 6 the XY-trajectory, the path following error, the steering angle and the yaw rate are shown for the vehicle controlled by the CarSim driver model and by the proposed control. To emphasize the simulation results only a detail of the path following manoeuvre is depicted as shown in the first subplot of Fig. 6: in that curve the vehicle reaches a lateral acceleration of 7.8 $[m/s^2]$. Both controllers achieve the path following however, as shown in the second subplot of Fig. 6, we may observe a more accurate lane keeping and a reduced path following maximum error in the lateral direction of 70% obtained by the proposed control law.

To analyze the performance of the proposed controlled system with respect to tire-road adherence variations a μ-split braking manoeuvre is performed ($\mu = 0.1$ on the left hand side and $\mu = 0.8$ on the right hand side in the CarSim model). A sudden braking action of 15 $[MPa]$ at a velocity of 40 $[m/s]$ is given on both the vehicle with the MPC and the vehicle with the nested PID control strategy: the proposed control system ensures the lane keeping (first subplot of Fig. 7) while the vehicle controlled by the CarSim driver model leaves the lane. The CarSim steering action saturates at the maximum allowed mechanical constraint that is equal to 720 $[deg]$ (12.56 $[rad]$ in Fig. 7) while we may observe the oscillations on the steering signal, provided by the proposed control, due to the ABS that prevents wheel lock while ensuring greater decelerations (third subplot of Fig. 7).

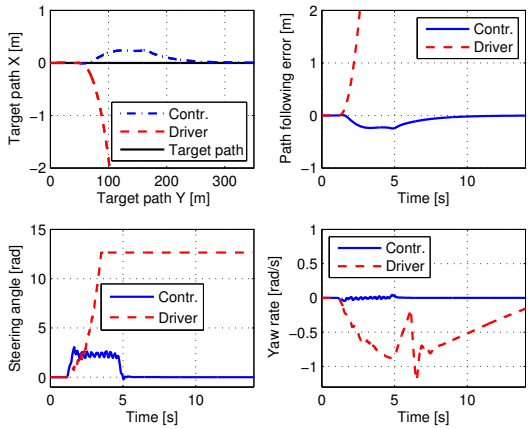

Fig. 7. μ-split braking manoeuvre

V. Conclusions

A vision based lane keeping control for autonomous vehicles has been proposed: as a first step, on the basis of lateral displacements at a look ahead distance provided by a vision system, a reference yaw rate signal is designed using PID control techniques; as a second step the steering angle is designed as a PI control on the yaw rate tracking error. The robustness of the proposed control with respect to speed variations and parameter uncertainties such as mass, front and rear cornering stiffnesses has been analyzed. Simulations in the CarSim environment illustrate the performance achieved by the proposed lane keeping control strategy both on a standard path and during a μ-split braking manoeuvre. The proposed controller is compared with the MPC used in CarSim as steering control which also requires the vehicle lateral speed and orientation: a reduced lateral offset and new stable μ-split braking manoeuvres are obtained by the proposed controller. Future work will explore the interactions of the proposed controller with the driver both during normal driving and in emergency conditions.

REFERENCES

[1] N. M. Enache, M. Netto, S. Mammar, B. Lusetti. Driver Steering Assistance for Lane Departure Avoidance. Accepted for publication in Control Engineering Practice, 7 October 2008.

[2] N. M. Enache, S. Mammar, M. Netto. Driver Steering Assistance for Lane Departure Avoidance Based on Hybrid Automata and on Composite Lyapunov Function. Accepted for publication in IEEE Trans. on Intelligent Transportation Systems, January 28, 2008.

[3] T. Raharijaona, G. Duc, S. Mammar. H_∞ Controller Synthesis and Analysis with Application to Lateral Driving Assistance. IFAC Symposium on Advance in Automotive Control, Salerno, Italy, April 2004.

[4] J. Kang, R. Y. Hindiyeh, S. Moon, J. C. Gerdes, K. Yi. Design and Testing of a Controller for Autonomous Vehicle Path Tracking Using GPS/INS Sensors. Proceedings of the 17th IFAC World Congress, Seoul, Korea, July 6-11, 2008.

[5] V. Cerone, M. Milanese, D. Regruto. Combined Automatic Lane Keeping and Driver's Steering Through a 2-DOF Control Strategy. IEEE Transactions on Control Systems Technology, Vol. 17, No. 1, pp. 135-142, Jan. 2009.

[6] V. Cerone, A. Chinu, D. Regruto. Experimental results in vision-based lane keeping for highway vehicles. Proceedings of the American Control Conference. Anchorage, AK May 8-10, 2002.

[7] C. Hatipoğlu, K. Redmill and Ü. Özgüner. Steering and Lane Change: A Working System. IEEE Conf. on Intelligent Transportation Systems, pp. 272-277, Boston, MA, 1997.

[8] C.C. MacAdam. Application of an Optimal Preview Control for Simulation of Closed-Loop Automobile Driving. IEEE Transactions on Systems, Man, and Cybernetics, Vol. 11, pp. 393-399, June 1981.

[9] P. Falcone, F. Borrelli, J. Asgari, H. E. Tseng and D. Hrovat. Predictive Active Steering Control for Autonomous Vehicle Systems. IEEE Transactions on Control Systems Technology, Vol. 15, NO. 3, pp. 566-580, May 2007.

[10] A. Takahashi, N. Asanuma. Introduction of HONDA ASV-2 (Advanced safety Vehicle-Phase 2). Proceedings of the IEEE Intelligent Vehicles Symposium. Dearborn (MI), USA, October 3-5, 2000.

[11] A. Broggi, M. Bertozzi, A. Fascioli, C.G. Lo Bianco, A. Piazzi. The ARGO Autonomous Vehicle's Vision and Control Systems. International Journal of Intelligent Control and Systems. Vol. 3, No. 4, pp. 409-441, 1999.

[12] T. B. Foote, L. B. Cremean, J. H. Gillula, G. H. Hines, D. Kogan, K. L. Kriechbaum, J. C. Lamb, J. Leibs, L. Lindzey, C. E. Rasmussen, A. D. Stewart, J. W. Burdick, and R. M. Murray. Alice: An information-rich autonomous vehicle for high-speed desert navigation. Journal of Field Robotics, Vol. 23, No. 9, pp. 777-810, Sept. 2006.

[13] M. Montemerlo, S. Thrun, H. Dahlkamp, D. Stavens, A. Aron, J. Diebel, P. Fong, J. Gale, M. Halpenny, G. Hoffmann, K. Lau, C. Oakley, M. Palatucci, V. Pratt, P. Stang, S. Strohband, C. Dupont, L.-E. Jendrossek, C.Koelen, C.Markey,C.Rummel,J.vanNiekerk, E. Jensen, P. Alessandrini, G. Bradski, B. Davies, S. Ettinger, A. Kaehler, A. Nefian, and P. Mahoney. Stanley: the robot that won the DARPA grand challenge. Journal of Field Robotics, Vol. 23, No. 9, pp. 661–692, Sept. 2006.

[14] L. Liu, M. Nagai, P. Raksincharoensak. On Torque Control of Vehicle Handling and Steering Feel for Avoidance Maneuver with Electric Power Steering. Proceedings of the 17th IFAC World Congress, Seoul, Korea, July 6-11, 2008.

[15] G. Baumgarten. Motor Vehicle Steering System Having a Yaw Rate Controller, Bayerische Motoren Werke. United States Patent Pub. No. US 20040070268 April 15/2004.

[16] A. Pauly, G. Baumgarten. Overlay Steering System and Method for Motor Vehicles, Bayerische Motoren Werke. United States Patent Pub. No. US 6854558 Feb 15/2005.

[17] Jurgen Ackermann. Robust Control. Springer, London 2002.

[18] M. Vidyasagar, H. Kimura. Robust Controllers for Uncertain Linear Multivariable Systems. Automatica, Vol. 22, No. 1, pp. 85-94, 1986.

[19] S. Paoletti, O.M. Grasselli and L. Menini. A Comparison Between Classical Robust Stability Conditions. International Journal Robust and Nonlinear Control, Vol. 14, pp. 249-271, 2004.

[20] H.B. Pacejka, Tire and Vehicle Dynamics. Elsevier - Butterworth Heinemann, 2004.

[21] C. Ching Yu and W. L. Luyben. Conditional stability in cascade control. Industrial & Engineering Chemistry Fundamentals, Vol. 25, No. 1, pp. 171-174, 1986.

VI. APPENDIX

TABLE I

VEHICLE NOMENCLATURE:

v	vehicle velocity	$v_{x,y}$	long. lateral speed
r	vehicle yaw rate	β	vehicle sideslip angle
a_y	lateral acceleration	c_a	aerodynamic coeff.
δ_p	driver steering angle	δ_f	front steering angle
m	vehicle mass	J	vertical axle inertia
l_f	front axle-CG dist.	l_r	rear axle-CG dist.
l_s	look ahead distance	μ	adherence coefficient
$f_{l,s}$	log./lateral forces	ρ	road curvature
$\alpha_{f,r}$	tire sideslip angle	$c_{f,r}$	cornering stiffness
$B_{f,r}$	Pacejka parameter	$C_{f,r}$	Pacejka parameter
$D_{f,r}$	Pacejka parameter	$E_{f,r}$	Pacejka parameter

TABLE II

VEHICLE PARAMETERS FOR THE LINEAR MODEL (6):

m	2023	[kg]	J	6286	[kg m^2]
l_f	1.26	[m]	l_r	1.90	[m]
c_f	2.864e+5	[N/rad]	c_r	1.948e+5	[N/rad]

TABLE III

SUBSTITUTIONS

$a_{c11} = a_{11}$ $\quad a_{c12} = a_{12} - K_{P1} b_1$

$a_{c14} = -\frac{K_{P1} b_1 (K_{P2}\tau + K_d)}{\tau}$ $\quad a_{c15} = -b_1 K_{I1}$

$a_{c16} = -\frac{K_{P1} b_1 K_{I2}}{\tau}$ $\quad a_{c17} = -\frac{K_{P1} b_1 (K_{I1} + K_{I2}\tau)}{\tau}$

$a_{c18} = -\frac{K_{P1} b_1 (K_{I1}\tau^2 - K_d)}{\tau^2}$ $\quad a_{c21} = a_{21}$

$a_{c22} = a_{22} - K_{P1} b_2$ $\quad a_{c24} = -\frac{K_{P1} b_2 (K_{P2}\tau + K_d)}{\tau}$

$a_{c25} = -b_2 K_{I1}$ $\quad a_{c26} = -\frac{K_{P1} b_2 K_{I2}}{\tau}$

$a_{c27} = -\frac{K_{P1} b_2 (K_{I1} + K_{I2}\tau)}{\tau}$ $\quad a_{c28} = -\frac{K_{P1} b_2 (K_{I1}\tau^2 - K_d)}{\tau^2}$

$a_{c54} = \frac{K_{P2}\tau + K_d}{\tau}$ $\quad a_{c56} = \frac{K_{I2}}{\tau}$

$a_{c57} = \frac{K_{I1} + K_{I2}\tau}{\tau}$ $\quad a_{c58} = \frac{K_{I1}\tau^2 - K_d}{\tau^2}$

TABLE IV

SUBSTITUTIONS

$h_7 = 1251.7$ $\quad h_6 = 7.4\ 10^5$ $\quad h_5 = 582\ 10^5$ $\quad h_4 = 3981\ 10^5$

$h_3 = 11231\ 10^5$ $\quad h_2 = 7434\ 10^5$ $\quad h_1 = 1373\ 10^5$ $\quad h_0 = 1.3\ 10^5$